Transactions of the Institute of Measurement and Control 29, 5 (2007) pp. 431–451

Advances in infrared technology for the online monitoring of injection moulding: application to the understanding of the nature of contact at the polymer–mould interface

A. Bendada[1], A. Derdouri[2], Y. Simard[2] and M. Lamontagne[2]

[1]Department of Electrical and Computer Engineering, Laval University, Quebec Quebec G1K 7P4, Canada
[2]National Research Council Canada, 75 De Mortagne, Boucherville Quebec J4B 6Y4, Canada

We describe a novel online infrared method for remote sensing of the surface and the bulk temperatures of polymers during injection moulding. The method may also be applied to other polymer forming processes such as extrusion and blow moulding. The key feature of the new method is the use of a hollow optical fibre that is incorporated into the injection mould to transmit the thermal radiation from the target to the sensor. The main characteristic of the hollow optical fibre is that it exhibits low transmission loss of the thermal energy in the mid- and far-infrared, and no end reflection. This allows measurement of quite low temperatures, as low as near room temperature. Conventional optical fibre thermometers can neither measure such low temperature ranges nor measure the polymer surface temperature. In this article, we present the first online results of critical tests of the new device. A Husky injection moulding press was used for the experiments. Good correlation was found between the radiometric

Address for correspondence: A. Bendada, Department of Electrical and Computer Engineering, Laval University, Pavillon Adrien-Pouliot, Local 1114-M, Quebec, Quebec G1K 7P4, Canada. E-mail: bendada@gel.ulaval.ca
Figures 1, 2, 5, 7 and 10 appear in colour online: http://tim.sage.pub.com

 10.1177/0142331207075587

results and those obtained with a thermal probe inserted near the polymer–mould interface, and with infrared imaging after the polymer part was ejected from the injection mould. In the second part of the paper, we show how the new infrared device can be used to give a better insight on the time evolution of the thermal contact between polymer and mould through the different phases of a typical injection moulding cycle. The experimental results show that thermal contact between polymer and mould is not negligible and not constant with time.

Key words: infrared waveguide; injection moulding; pyrometry; radiometry; temperature; thermal contact resistance; thermal probe.

1. Introduction

In polymer processes such as extrusion, injection moulding or blow moulding, the material undergoes a complex history in which it is melted, flows through complex geometries where viscous dissipation, shrinkage and warpage play a central role, is deformed to take the shape of the mould, and finally is cooled down and solidified into the final product. In all these processes, temperature distribution in the polymer is extremely complex and has a significant effect on the properties of the final part as well as the cycle time. Temperature is probably one of the most important parameters in polymer forming. However, its measurement is extremely difficult. One of the difficulties is the nature of the processes in which the material moves and solidifies to form the product so that invasive techniques such as thermocouple insertion are not applicable. Another difficulty is the existence of non-uniform temperature throughout the melt thickness (Lai and Rietveld, 1996; Migler and Bur, 1997). Products that are moving or too fragile to touch are easily measured with non-contact techniques. Previous attempts to remotely measure the temperature include the use of fluorescence spectroscopy (Migler and Bur, 1998), ultrasonics (Konno *et al*., 1993) and infrared pyrometry (Maier, 1996). In the fluorescence spectroscopy method, a temperature sensitive dye is incorporated into the polymer at dopant levels and the local temperature is measured by monitoring spectral features of the dye. In the ultrasonic technique, ultrasonic velocity in a hot body is converted to temperature by means of a precisely measured velocity–temperature relation. In infrared pyrometry, the radiant energy emitted by the polymer is used to retrieve the temperature inside the material. In this work, we describe an original radiation thermometer for polymer temperature sensing.

Radiation thermometers have been used to measure process stream temperatures for some time in processing industries such as the steel industry, the aluminium industry and the glass industry. However, in the field of polymer processing, the application of radiation thermometry has drawn only a limited amount of attention from researchers, and its successful application to measure either bulk or detailed process stream temperatures remains a challenging task. Due to the restricted theoretical developments as well as hardware limitations, applying radiation thermometers has at present only been able to provide thermal information about

the process stream in terms of an average or bulk temperature, but not about the detailed temperature distribution inside the polymer melt. Beyond the limitation to bulk temperature measurements, another serious drawback of the present thermometers is their limitation to high-temperature targets (eg, $T > 120^{\circ}C$). This is due to the limited transmission behaviour of the employed optical fibres to the visible and the near-infrared spectral bands. Mid- and far-infrared optical fibres do exist (such as fluoride and chalcogenide glasses) but they are expensive, very fragile and therefore not appropriate for harsh industrial environments (Saito and Kikuchi, 1997).

To carry out remote low-temperature radiometry in the polymer processing industry, we devised a new radiometric unit based on the employment of a dielectric-coated silver hollow optical fibre (Harrington, 2000; Matsuura and Harrington, 1995). In radiation thermometry below 120°C, the dielectric coated metallic hollow optical fibre holds transmission efficiency to as high as 50%. The hollow optical fibre consists of silver and dielectric films deposited on a glass supporting tube. As long as mechanical flexibility is not required for the radiation guide, the dielectric-coated hollow optical fibre is the preferred choice for remote thermometry in lower temperature ranges. To date, the hollow optical fibre technology has mainly been used in infrared laser delivery systems including laser surgery and material processing (Cossman *et al*., 1995; Gannot *et al*., 1995). Its use in thermometry has been limited to a few laboratory experiments, using blackbody sources, aiming to investigate the ability of hollow optical fibres to monitor low temperatures (Alaluft *et al*., 1993; Saito *et al*., 1992). The new radiometric unit was designed to measure the bulk temperature inside the polymer, as well as the polymer surface temperature. This new approach is based on the polymer semi-transparency in the spectral band of the photon detector, and on the temperature gradient within the polymer thickness. Thermal information at the polymer surface is a particular advantage of the new radiometric system over commercially available thermometers. This advantage may be useful to obtain a better understanding of the nature of thermal contact between polymer and mould (Delaunay *et al*., 2000; Quilliet *et al*., 1997), or to get rid of background spurious energy emissions in thin polymer streams (see Section 2). Surface temperature measurement may also be employed to retrieve the detailed temperature profile through the polymer thickness using algorithms for ill-posed inverse problems (Bendada and Nguyen, 1999; Nguyen and Bendada, 2000; Rietveld and Lai, 1994).

2. Radiation thermometry of polymers

Radiation thermometry in the polymer industry involves the evaluation of the spectral emission characteristics of the polymer to be measured. The energy emitted by a polymer material is not evenly distributed in the infrared spectrum. Polymers are spectrum-selective materials (Lai and Rietveld, 1996; Migler and Bur, 1997). By observing the wavelengths at which peak energy is emitted, an instrument sensitive to that wavelength can be selected. This selection is most critical for thin-film

polymers for which the thermal radiation detected by the infrared probe is generated not only from the melt polymer film, but also from the surrounding solid surface or background. Selection of the wavelength of peak energy emission is also critical for surface temperature measurement of thicker polymers when the temperature profile through the film thickness is not uniform. For example, polypropylene is partially transparent [about 75% (τ)] at most wavelengths between 2 and 16 μm except for a few wavelengths at which strong absorption bands exist. Figure 1 shows the overall transmission spectrum of 25- and 250-μm thick polypropylene specimens. A fundamental carbon–hydrogen (C–H) absorption band at 3.4 μm causes transmission to be zero. From an infrared radiometric point of view, this represents a special region where thin plastic films are opaque. Using an infrared thermometer with a selective narrow band filter in this region, it is possible to measure the film surface temperature accurately rather than the combination of the film and background temperatures. Thus, using the transmission data of Figure 1 and assuming a reflectance of 4% (ρ), emissivity (ε) can be calculated for polyethylene at 3.4 μm: $\varepsilon = 1 - \rho -$, or $1 - 0.04 - 0 = 0.96$. Since τ decreases and ε increases as thickness increases, thermometer spectral response becomes less important with thicker polymer films, unless there is a need to measure the surface temperature. In general, thicknesses of less than 2.5 mm require consideration of spectral emission, which should be analysed with a spectrometer to determine the best wavelengths for non-contact temperature measurement. Similarly, in the case of polyester and other ester related polymers, there is a strong C–O absorption band at 7.9 μm, whereas fluoro-polymers show strong C–F absorption in this region. In measuring these films, it is necessary to use a radiometric sensor with a selective narrow-band filter at 7.9 μm. Some polymers can be measured only at 3.4 μm and some can be measured only at 7.9 μm, while others can be measured at either wavelength. The three polymer groups are listed below:

3.4 μm	3.4 μm or 7.9 μm	7.9 μm
Polyamide	PVC	Polyester
Polyethylene	Acrylic	PTFE
Polypropylene	Polyurethane	Polyimide
Polystyrene	Polycarbonate	Cellophane
Nylon		Cellulose acetate
Ionomer		Fluoroplastic
Polytbutylene		
Glassine		

In the present work, we only consider the conception of a thermometer able to detect the radiation emitted in the 3.4-μm spectral region. The thermometer may operate either with or without a narrow band pass (NBP) filter at 3.4 μm to measure

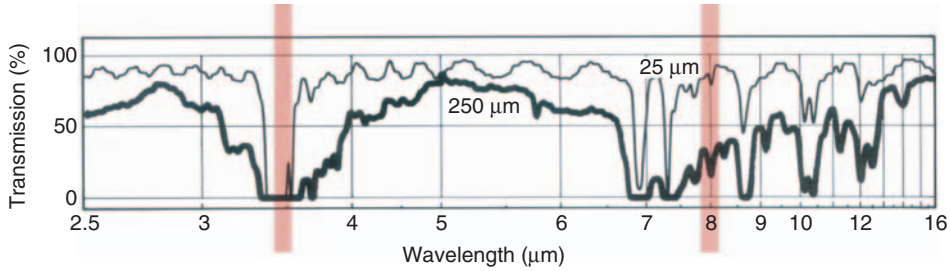

Figure 1 Transmission spectra of 25- (thin solid line) and 250-μm thick (bold solid line) specimens of polypropylene. Polypropylene exhibits an absorption peak at 3.4 μm, whereas it is transparent at 7.9 μm

either the surface or bulk temperature of a polymer film. For surface temperature measurement, the thermometer can be operated only for the polymers of the first or second group listed above. A radiometric unit sensitive to the 7.9-μm wavelength band may be similarly designed for surface temperature measurements of polymers of the second and the third groups above.

3. Radiation thermometer design

A thermometry system, using a dielectric-silver-coated glass hollow optical fibre, was devised and examined for continuous operation in an injection moulding process. One can assume for this kind of application that the polymer stream temperature is mainly between 30 and 300°C. The infrared system consists of a detector head, sensing probe containing a hollow optical fibre and signal-processing unit.

Figure 2 is a diagram of the probe installed in the mobile side of the injection mould along with the detector head. The hollow optical fibre, incorporated inside the ejection pin, gathers the thermal radiation emitted from the hot polymer and transmits this energy to the photon detector. The employed hollow optical fibre consists of a silver film deposited on the inside of a smooth glass supporting tube, and a single fluoro-carbon-polymer (FCP) film that is transparent at the desired wavelength. It was manufactured and optimized to meet our needs by a research group at Tohoku University. The concept of this type of hollow optical fibre is based on the fact that though metal-tubing fibres exhibit high attenuation, an inner dielectric coating that is properly designed reduces the attenuation loss drastically. The optimum thickness of the dielectric film depends on its refractive index and the desired wavelengths to be transmitted (3.4 m spectral region in the current study). A schematic illustration of the cross structure of a hollow optical fibre after deposition of the guiding layers is shown in Figure 3. The hollow optical fibre has an inner diameter of 4 mm, an external diameter of 6 mm and a length of 40 cm. Its transmission losses are smaller

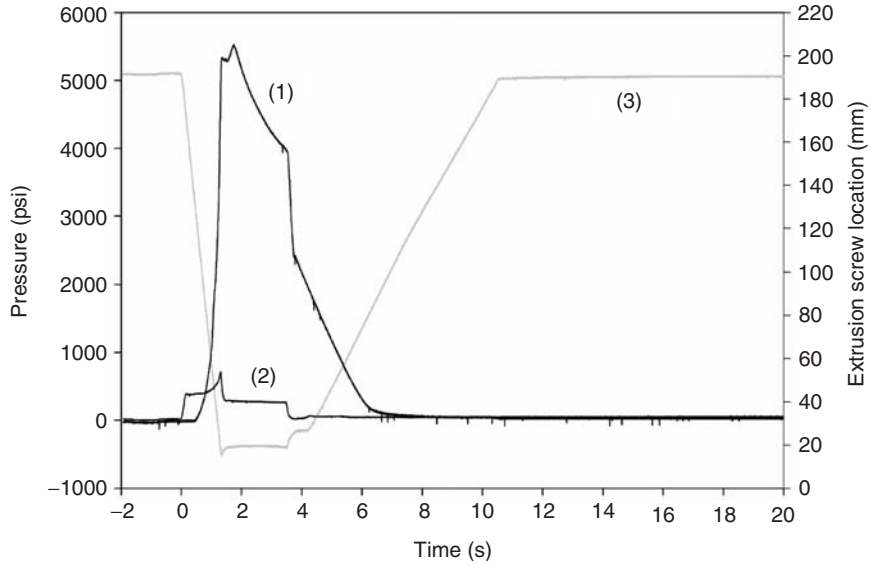

Figure 2 Geometry details of the hollow optical fibre thermometer inserted into the moving half-mould side

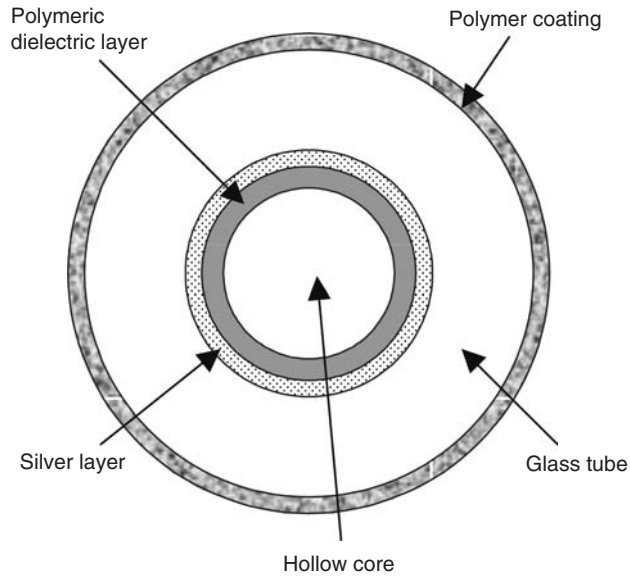

Figure 3 A schematic illustration of a hollow optical fibre cross-section showing the tube and the guiding layers

than 2 dB/m in the 2–4-μm spectral range, so that the attenuation due to the employed 40-cm-long pipe portion is quite acceptable. A Teflon sleeve is inserted between the hollow optical fibre and the inside of the ejection pin to absorb mechanical shocks. The hollow optical fibre is coupled directly to the detector cell-housing window. The direct coupling is quite efficient, but may be improved by inserting an optical lens between the detector head and the hollow optical fibre face.

The probe is an ejection pin made with the same P20 steel grade as the mould material. It is machined through its axis to contain the hollow optical fibre. It plays the role of shielding the hollow optical fibre from mechanical shocks and excessive temperature increase. A circular cavity (diameter 10 mm, depth 2 mm) is machined at one end of the ejection pin to house a flat sapphire window. Sapphire is selected because it is transparent in the 3.4-μm wavelength region, strong at high temperatures and good for high-pressure applications. The window thickness was calculated to withstand the high pressure inside the mould cavity (Chervin *et al*., 1994), namely ∼50 MPa. An Epotek 353ND epoxy adhesive designed for high-temperature and pressure applications is employed for assembling the optical window to the ejection pin. The probe is inserted into the injection mould so that the tip of the sensor is flush with the inside cavity surface. The other end of the probe is designed to be connected to the detector head, which in turn is connected to the signal processing unit.

The thermal energy transmitted through the hollow optical fibre is imaged onto a Judson Technologies Indium Arsenide (InAs) photovoltaic detector. The latter is sensitive in the 1.0–3.6-μm spectral region, with a peak sensitivity at 3.4 μm. This spectral response is very convenient for monitoring polymers of the first and second groups, which exhibit high energy emission at 3.4 μm. The photodiode is mounted with thermistors on two-stage thermoelectric coolers and hermetically sealed in a dry nitrogen environment. In order to get a high detectivity, good stability over the required temperature excursion range and a cut-off wavelength at 3.5 μm, the detector is cooled down to a temperature of −30°C. A preamplifier that converts the current output of the detector into a voltage output is used with a 200-kHz bandwidth and a 10^4 V/A gain. The temperature is inferred from the detector output through a calibration curve as discussed below.

A NBP filter transparent to the 3.4-m wavelength through a 140-nm half bandwidth is inserted between the hollow optical fibre and the detector to isolate the radiation emitted by the hot polymer surface. The optical filter is employed only when surface temperature measurement is required. Removing the filter allows measuring the average temperature through a certain optical penetration depth in the polymer. However, in this operating configuration, the spurious radiation emitted by the opposite mould side may affect the measurement of thin polymer streams.

Prior to carrying out online trials, the radiometric device was calibrated using a Mikron M315 blackbody source in the temperature range 30–300°C. Calibrations were performed with and without insertion of the NBP filter at room temperature (Figure 4). To investigate the effect of the hollow optical fibre temperature on the

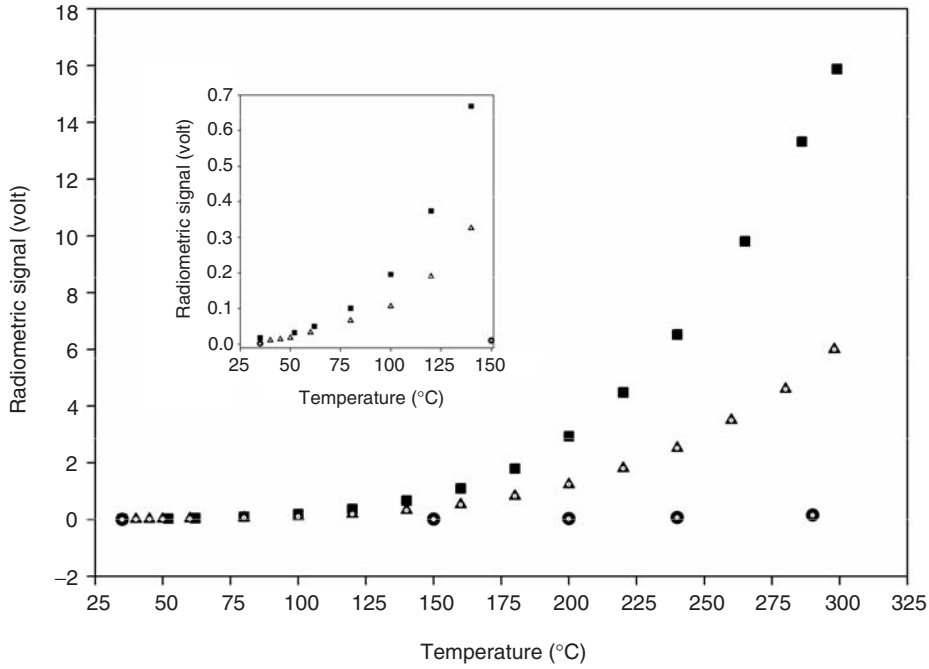

Figure 4 Relation between the thermometer and blackbody temperature. Squares show the calibration when the optical filter is not inserted into the probe. Triangles show the calibration when an optical filter is inserted into the probe. Circles show for reference the calibration with a highly reflective stainless steel tube

calibration curve, the experiment was again performed after holding the hollow optical fibre in an oven at variable temperatures (<80°C). The hollow optical fibre transmission was not affected by its elevated temperature. We also analysed for reference purposes the usefulness of the FCP-silver-coated glass pipe over the use of a highly reflective metal tube. We performed a comparison calibration using a stainless steel tube without NBP filter insertion. It is obvious from Figure 4 that the dielectric-metal-coated hollow optical fibre enhances drastically the sensitivity of the remote infrared system in low-temperature radiometry.

4. Experimental validation of the new radiation thermometer

The experiments were carried out on a 250-ton Husky injection moulding press. Images in Figure 5 show the detailed shape of the manufactured polypropylene part. Polypropylene was selected because it exhibits a peak absorbance at the 3.4-μm wavelength. This characteristic is useful to test the ability of the new

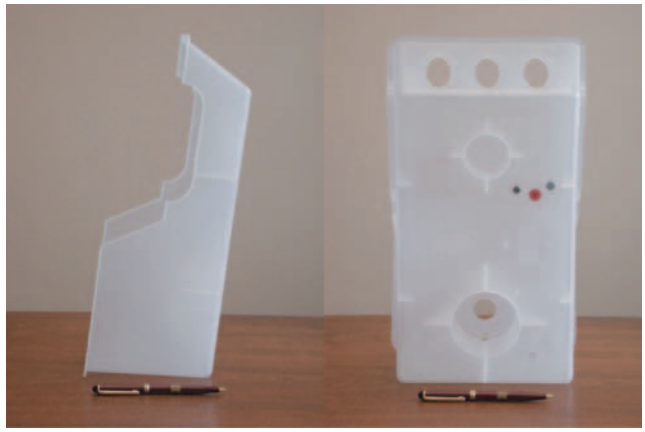

Figure 5 Shape of the injected polypropylene part and corresponding locations of the thermal probe (circle on the left side), the hollow optical fibre probe (circle in the centre) and the cavity pressure transducer (circle on the right side)

radiometric device in measuring the temperature at the polymer surface. Another reason that motivated the choice of polypropylene is related to its high sensitivity to temperature and inside cavity pressure ranges. Shrinkage and warpage phenomena are in general quite significant for polypropylene during injection moulding (Delaunay *et al.*, 2000; Quilliet *et al.*, 1997). The nominal thickness of the experimental injected part is 2.3 mm, which is quite small compared to the lateral extension of the part. Such dimensions usually favour one-dimensional heat diffusion through the stream thickness in locations far from part non-homogeneities.

The hollow optical fibre radiometric unit described above was set into an experimental injection mould (Figure 2) to analyse temperature changes of the polymer flow during the process. The sensing probe was installed in such a way that the sapphire window was flush with the face of the mould cavity. In order to investigate the effect of process conditions on the temperature reading, two other sensors were incorporated beside the infrared probe. Figure 5 shows the relative locations of the three sensors with coloured circles painted on the injected part. The large circle in the centre shows the area where the infrared probe collected the thermal radiation. On the right-hand side, a D.M.E SS-405C standard slide pressure transducer was inserted to record the inside cavity pressure. On the left-hand side, a thermal probe, which was designed specially in our laboratory for this study, was inserted to monitor the temperature at the mould surface. Data acquisition for all sensors was performed at a frequency rate of 500 Hz so that rapid and sudden signal changes could be observed.

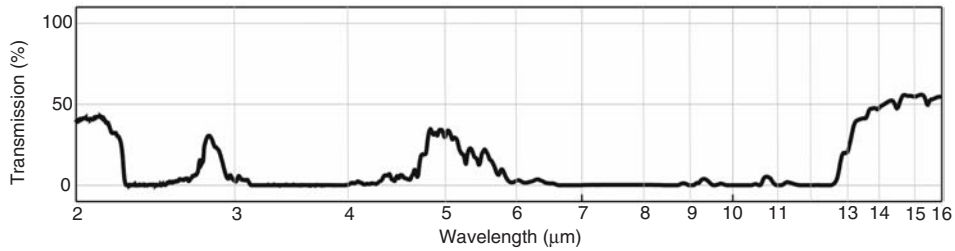

Figure 6 Transmission spectrum of a 2.3-mm-thick polypropylene film. The film is still semi-transparent in the sensitive spectral range of the InAs detector, and opaque in the infrared camera 9-μm region

During the experiments, the operating parameters, such as injection temperature, hydraulic pressure, mould-cooling-oil temperature and extrusion screw movement, were also carefully monitored. Meanwhile the press was kept running in order to maintain it in a stable condition. The hydraulic pressure was set to its lowest level to favour polymer shrinkage and unsticking phenomena at the polymer–mould interface. Numerous series of experiments were undertaken for different combinations of the process parameters. In each series, the hollow optical fibre radiometric unit was employed with or without the optical filter in order to obtain either the surface or the bulk temperature of the polymer stream. For the sake of clarity, only the results for one trial series will be reported in the current article. The series concerned corresponds to a mould-cooling-oil temperature of 25°C, and an injection melt temperature of 275°C.

Since the polymer part thickness was quite small, namely 2.3 mm, the bulk temperature reading might be affected by the background radiation emitted by the opposite side of the mould cavity. This issue was investigated with the overall transmission spectrum of a 2.3-mm thick polypropylene film as recorded by a standard FTIR spectrometer. Spectral scans (Figure 6) revealed that the 2.3-mm thick film is still partially transparent in the sensitive range of the InAs detector. The magnitude of the error introduced by the spurious radiation on the bulk temperature measurement would obviously depend on the polymer and mould temperature levels.

For reliability investigation, the temperature recorded with the hollow optical fibre device just before the part was ejected out of the mould was compared to the temperature recorded with an Agema 900 LW infrared camera when the part was outside the mould. A few seconds passed between the time the part was ejected and thermal imaging performed. This delay was related to the time necessary to bring the ejected part in front of the thermography unit. This had a HgCdTe detector sensitive in the 4–14-μm spectral band. To avoid having the imaging system capture the background radiation, a NBP filter centred at 9.0 μm was incorporated into the optical field of view of the camera detector. The use of the latter filter is

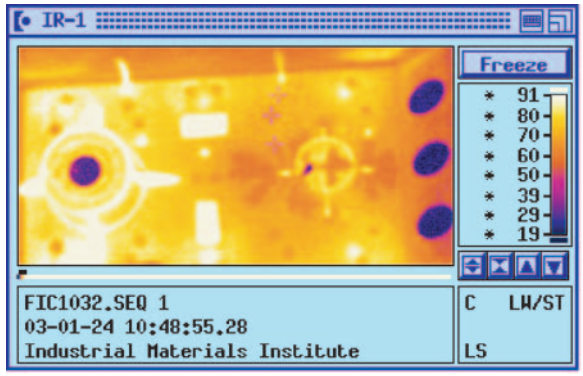

Figure 7 Typical infrared image of the polypropylene part after it is ejected out of the injection mould

justified by the transmission spectrum of the 2.3-mm-thick polypropylene film reported in Figure 6. The 2.3-mm-thick part is completely opaque in the 9.0-μm wavelength region. Figure 7 shows a typical infrared image of the polypropylene part after it is ejected out of the injection mould. The three crosses on the image show the corresponding locations of the thermal, infrared and pressure sensors. The temperature at the location of the hollow optical fibre probe was extracted from the thermal image and then reported in Figure 8 together with the surface and bulk temperature histories of the part obtained with the hollow optical fibre thermometer. The hollow optical fibre thermometer data were also compared, on the same graph, to the temperature history of the mould at the cavity surface by the thermal probe. Hydraulic pressure, inside cavity pressure and extrusion screw location recorded during the same injection cycle are reported in Figure 9.

The following observations deserve to be pointed out:

- During the filling and the cooling under pressure, a good contact is ensured between the polypropylene and the mould, so the heat transfer occurs across a small thermal contact resistance (TCR). As soon as the relative pressure becomes equal to zero, the effect of the shrinkage results in the appearance of an air gap between the mould and the polymer. This air gap disturbs the heat transfer near the interface (Delaunay *et al*., 2000; Quilliet *et al*., 1997). A consequence of this bad heat transfer at the interface is a sudden drop in the heat flux density crossing the interface between the polymer and the mould. Indeed, the heat from the core of the part, which is cooling, is carried by conduction toward the polymer surface, and in case of good contact, crosses the interface to be evacuated in the mould. On the other hand, if an air gap suddenly occurs between the polymer and the mould, the polymer can be reheated at its surface and an abrupt hump can be seen on the temperature versus time curve. It can be clearly observed from Figure 8 that the surface polymer temperature history is more sensitive to the presence of an air gap than the bulk polymer temperature. In addition, the air gap causes the plastic part to cool more slowly, which is exactly observed in the bulk and surface temperature curves.

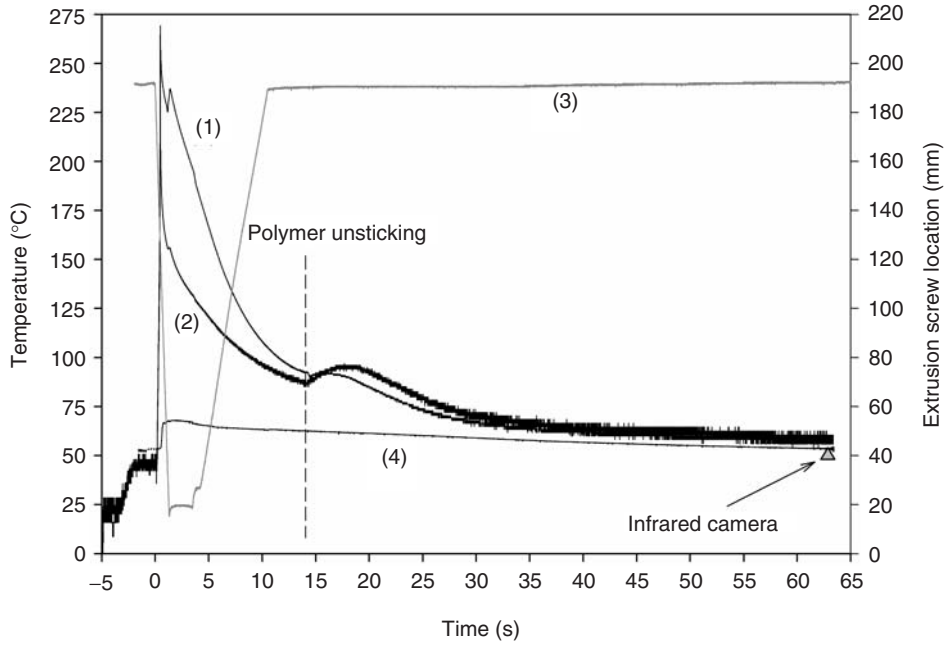

Figure 8 Temperature measurements of the polymer stream inside the cavity for a melt temperature of 275°C and a cooling oil temperature of 25°C. Curve (1): polymer bulk temperature; curve (2): polymer surface temperature; curve (3): location of the extrusion screw; curve (4): mould temperature near the cavity surface; grey triangle: thermography measurement

- The bulk temperature before the appearance of the air gap is greater than the surface temperature. This is due to the transparency of the polymer and a non-uniform temperature profile through the stream thickness. The temperature in the core is higher than at the surface. The infrared probe's reading is dominated by the hot material at the core of the cavity and the opposing wall makes a relatively insignificant contribution toward this measurement. When the polymer becomes unstuck from the cavity surface, the relative behaviour of the bulk and surface temperature is reversed. The surface temperature becomes slightly higher than the bulk temperature. This might be caused by the fact that at that temperature magnitude the error introduced into the bulk temperature by the radiation emitted from the opposite mould cavity side is significant. After the sudden temperature increase, the deviation between the surface and bulk temperatures reduces to become insignificant at the end of the cycle. This is due to the fact that the temperature gradients through the polymer thickness are quasi-null, making the average temperature over the optical penetration depth equal to the surface temperature.
- The polymer stream reaches the infrared probe ~0.43 s after the injection cycle begins. It is the time of the maximum temperature (bulk or surface) rise. Time zero is known

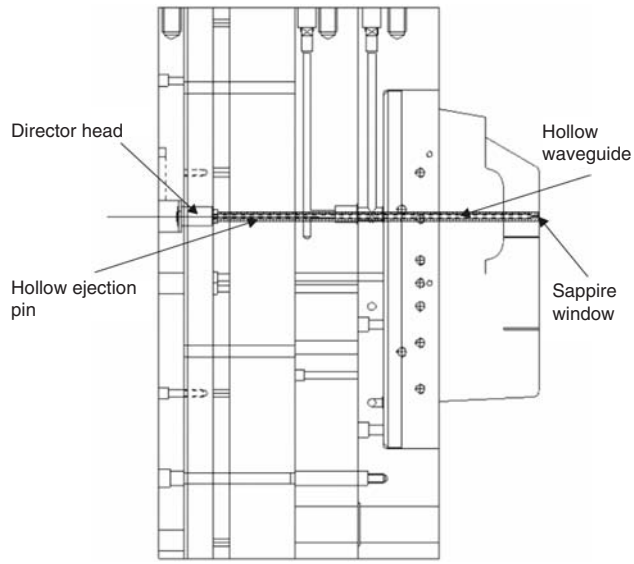

Figure 9 Inside cavity pressure (curve 1), hydraulic pressure (curve 2) and extrusion screw location (curve 3) during the injection cycle

through the extrusion screw movement reported by curve (3) in Figures 8 and 9. Between times 0 and 0.43 s the cavity in front of the infrared probe is empty; the temperature increase is only apparent. It is caused by the multiple reflections over the mould cavity walls of the radiation emitted from the hot polymer when it spurts out of the injection gates.

- The inside cavity pressure has a direct effect on the temperature of the polymer stream. The abrupt pressure fluctuation that occurs just before the pressure reaches a maximum affects instantaneously the temperature versus time curve. A temperature fluctuation occurs at the same moment the pressure fluctuation happens.
- The part temperature measured with thermography, a few seconds after the part was ejected from the mould is reported by the triangle in Figure 9. It is slightly lower than the polymer temperature measured with the hollow optical fibre thermometer just before the part is ejected. The reason for this discrepancy must be the delay between the ejection and thermography measurement. However, this measurement remains significant and useful, since it gives an idea on the reliability of the new radiometric unit.
- Another indication of the good reliability of the new radiometric unit is the temperature of the mould surface recorded with the thermal probe. Indeed, near the end of the injection cycle, the polymer temperature (surface or bulk) measured with the hollow optical fibre thermometer tends to catch up to the near surface mould temperature. The discrepancy that still remains at the end of the cycle is likely caused by a non-perfect contact between polymer and mould.

5. Application to the analysis of thermal contact between polymer and mould

This section describes how the hollow optical fibre thermometer can be used to characterize the nature of thermal contact between polymer and mould through the different phases of a typical injection moulding cycle. The key idea is the combination of the measurements provided by the new infrared device and a thermal probe to determine the TCR. The hollow optical fibre thermometer is used for the online monitoring of the temperature at the surface of the polymer stream, while the thermal probe is utilized to determine via an inverse heat conduction procedure the heat flux crossing the polymer–mould interface and the temperature at the cavity surface.

In injection moulding, the characterization of the thermal contact between polymer and mould and the prediction of its evolution with pertinent process parameters are very difficult. The reason is its dependence on boundary conditions that cannot be measured reliably using conventional procedures such as thermocouples and heat flux transducers that may affect the heat transfer at the interface. The TCR may be defined per surface unit as $\mathrm{TCR} = (T_{ps} - T_{ms})/\varphi$, where T_{ps} is the polymer surface temperature, T_{ms} is the mould surface temperature, and φ is the heat flux density crossing the interface. To determine polymer surface temperature T_{ps}, we used the hollow optical fibre thermometer described in Section 4. Mould surface temperature T_{ms} and heat flux density φ were indirectly obtained with the use of a specially designed thermal probe. Figure 10 shows an image of the probe. The latter was composed of two steel half-cylinders joined side by side. These were obtained by cutting longitudinally a cylinder that was 8 mm in diameter and 130 mm long. The shape and size of the cylinder tip in contact with the polymer stream were designed to fit commonly employed

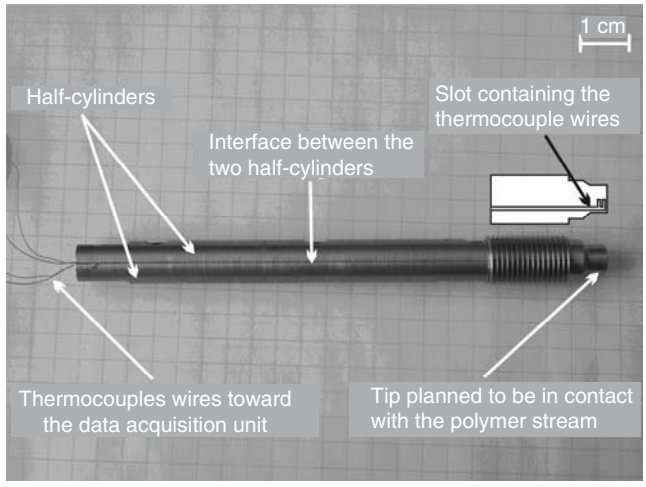

Figure 10 Image of the thermal probe

probe-housing cavities in injection moulds. Two *E*-type fine-wire thermocouples 75 μm in diameter were spot-welded inside and along the axis of the cylindrical probe at two different locations (1 and 2 mm) from the probe tip. At the interface between the two half-cylinders, a narrow slot was longitudinally machined in one half-cylinder to contain the thermocouples wires. The shape and the location of the slot are represented with a diagram in Figure 10. Two thermocouples, rather than a single thermocouple, were utilized because the additional information could aid in more accurately estimating the surface conditions via the sequential procedure detailed thereafter. To perform perfectly non-intrusive measurements, the thermal probe was manufactured with the same steel (P20 steel grade) as the mould material and the same roughness as the cavity surface. Two 3B47-conditioning modules from Analog Devices Company amplified the thermocouple signals to a data-acquisition system and control unit. The latter devices were piloted with a computer via a GPIB card. The 3B47 module allowed the automatic conversion of the monitored voltage to temperature. A signal processing software, Labtec, was used for the visualization and the exploitation of the experimental results.

From temperature histories monitored with the thermal probe, a regularized sequential inverse method allowed the estimation of both heat flux φ crossing the polymer–mould interface and temperature at the cavity surface T_{ms}. This data processing was based on Beck's method that used a combination of the function specification method and the future time steps concept (Beck *et al.*, 1985). Close to the polymer–mould interface, heat transfer in the mould can be assumed to be one-dimensional. The temperature field can thus be described by the variable $T(x,t)$. The mould is considered as a semi-infinite body (defined by $x \geq 0$) initially at temperature T_0; for times $t > 0$, there is heat generation at the mould surface ($x = 0$) at a rate of $q(t)$ per unit time, per unit surface. The mathematical formulation of this problem is given as

$$\frac{\partial^2 T(x,t)}{\partial x^2} = \frac{1}{\alpha}\frac{\partial T(x,t)}{\partial t} \quad \text{in } 0 < x < \infty,\ t > 0 \tag{1}$$

$$-\lambda \frac{\partial T}{\partial x} = q(t) \quad \text{at } x = 0,\ t > 0 \tag{2}$$

$$T = T_{\mathrm{o}} \quad \text{for } t = 0, \text{ in the region} \tag{3}$$

where α and λ are the thermal diffusivity and thermal conductivity of the mould material, respectively. The exact solution of the temperature field $T(x,t)$ can be analytically calculated with the use of Duhamel's theorem (Ozisik, 1980).

From temperature histories monitored with the two-thermocouple probe, a regularized sequential inverse method allows the estimation of both heat flux crossing the polymer–mould interface and temperature at the cavity surface. This data processing is based on Beck's method that uses a combination of the function specification method and the future time steps concept. It may be applied for one or a few micro-thermocouples. The detailed description of the method has been presented elsewhere (Beck, 1986; Beck *et al*., 1985), and only a brief account is given here.

In the function specification approach, the entire period in which the polymer is in contact with the mould is divided into a finite number of time intervals. The heat flux varies from one interval to another, but a constant value q_M is assumed within each individual interval $[t_{M-1}, t_M]$. The estimated heat flux components $q_1, q_2, \ldots, q_{M-1}$ are assumed to be known and the objective is to estimate q_M. In order to add stability to the inversion algorithm, the future time steps procedure is utilized as well. It assumes temporarily that several future heat fluxes are constant with time. Hence r future heat flux components are temporarily made equal. The optimized value of the heat flux is obtained in a sequential manner by increasing M by one for each time step in the following expression:

$$q_M = \frac{\sum_{i=1}^{r} \sum_{j=1}^{J} \left(Y_{j,\,M+i-1} - T_{j,\,M+i-1}|_{q_M=\ldots=q_{M+i-1}=0} \right) Z_{ji}}{\sum_{i=1}^{r} \sum_{j=1}^{J} Z_{ji}^2} \tag{4}$$

In this equation, the first subscript, j, refers to space (sensor number) and the second to time. There are r future times and J temperature sensors. $Y_{j,\,M+i-1}$ refers to a measured temperature by sensor number j at the time interval $[t_{M+i-2}, t_{M+i-1}]$, while $T_{j,\,M+i-1}$ is the exact temperature calculated by solving the forward problem, Equations (1)–(3), at the same location and time interval when fluxes $q_M, \ldots, q_{M+i-1}$ are set to zero. The quantities Z_{ji} are defined by

$$Z_{ji} = \sum_{k=0}^{i-1} X_{j,\,M+k}(t_{M+i-1}) \tag{5}$$

where $X_{j,\,M+k}(t_{M+i-1})$ represents the sensitivity coefficient of temperature calculated at the location of sensor number j at time t_{M+i-1} with respect to a heat flux component q_{M+k}, and is defined as

$$X_{j,\,M+k}(t_{M+i-1}) = \frac{\partial T_{j,\,M+i-1}}{\partial q_{M+k}} \tag{6}$$

The choice of the number of future times r is an important parameter for stabilizing the algorithm. Suitable conditions to choose r as a function of sampling time step and magnitude of measurement noise are given by Reinhardt (1993). Although the heat

fluxes are temporarily assumed to be constant for a period involving r future time steps, once the optimized value is obtained, it applies only for the time interval $[t_{M-1}, t_M]$. After the determination of the surface heat flux components, the surface temperature is simply calculated with the analytical solution of the forward problem described by Equations (1)–(3).

The accuracy of the calculations produced with the inversion algorithm was numerically assessed against the exact solution of a heat flux that varied in time in a triangular fashion. The solid line curve in Figure 11 illustrates the exact heat flux distribution. The test consisted in solving the heat transfer equation for the latter heat flux boundary condition and a uniform initial temperature field, $T_0 = 0$. Then, exact internal temperature distributions as a function of time at two different locations from the surface, namely 1 and 2 mm, were calculated. The solid line curve 1 in Figure 12 is the exact temperature at 2 mm from the surface, while the solid line curve 2 is the exact temperature at 1 mm from the surface. To make the validation test more realistic, random errors generated numerically were added to the exact temperatures. The resulting simulated noisy temperatures are plotted in the same graph with triangle and square symbols, respectively. Subsequently, these two simulated temperatures were used as 'experimental' inputs for the inverse heat conduction algorithm. The inversed heat flux and surface temperature are reported in Figures 11 and 12, respectively, with the black circle curves. The results are quite stable and a good agreement between exact (solid line curves) and inversed data can be clearly observed.

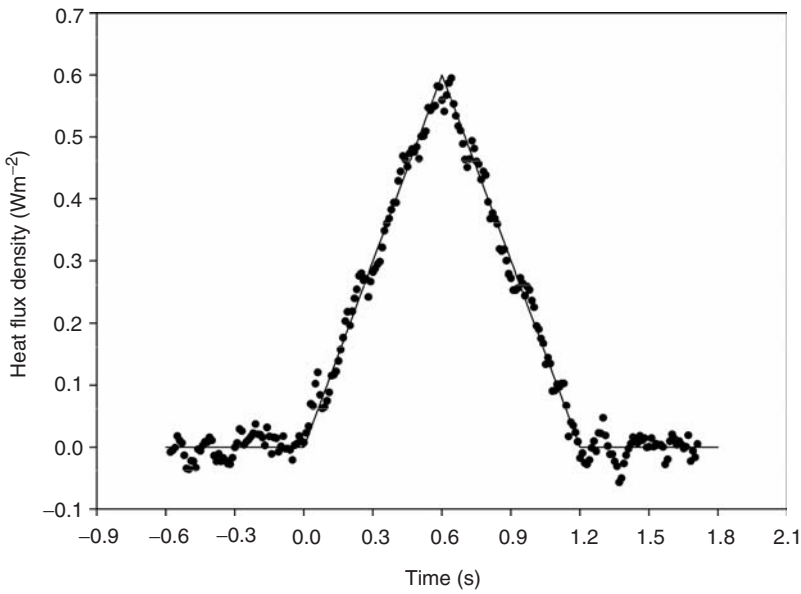

Figure 11 Comparison of the calculated surface heat flux (•) using Beck's method and the true heat flux data (—)

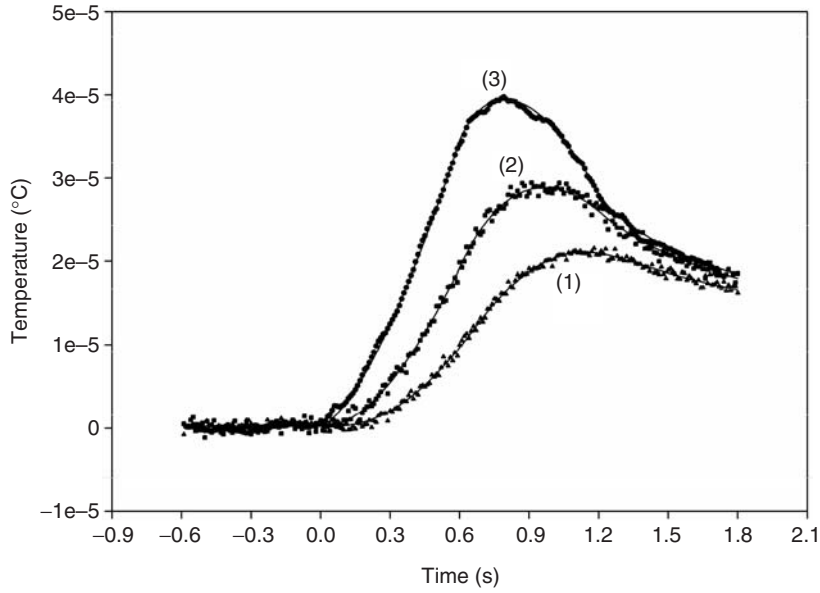

Figure 12 Calculated temperature at the surface of the mould (●) using the internal simulated noisy temperatures at a distance of 1 mm (■) and 2 mm (▲), respectively from the mould surface. The solid line (—) curves are the true temperature data obtained by the solution of the forward problem

After the theoretical validation of the inversion algorithm, experiments were carried out on the injection moulding machine. The plastication conditions were set so that an injection temperature of 220°C was achieved; the mould temperature was regulated at 25°C and the hydraulic pressure was set to 2.5 MPa. The injection rate was 11 cm/s, the packing time 1.75 s and the holding time 3.5 s.

During the cooling, as the solidification progressed, the part begun to shrink through its thickness and an air gap was likely to be formed at the polymer–mould interface. After a sizable gap was developed, the interface returned to the steel-air condition, and therefore, the pressure dropped back to its minimum level. As soon as the relative pressure became equal to zero (at ~12 s), the heat transfer near the interface was disturbed by the air gap appearance and led to a sudden rise of the surface temperature decay signal. This deviation is illustrated by curve 1 in Figure 13. In addition, the air gap caused the polymer part to cool more slowly, which is exactly observed in the slope change of the temperature history in Figure 13.

Typical evolutions of temperature in the mould, ie, temperatures measured with the thermal sensor, are represented by curves 2 and 3 in Figure 13. Curve 2 refers to the thermocouple located at 2 mm from the mould surface, while curve 3 refers to the thermocouple located at 1 mm from the mould surface. The mould surface temperature

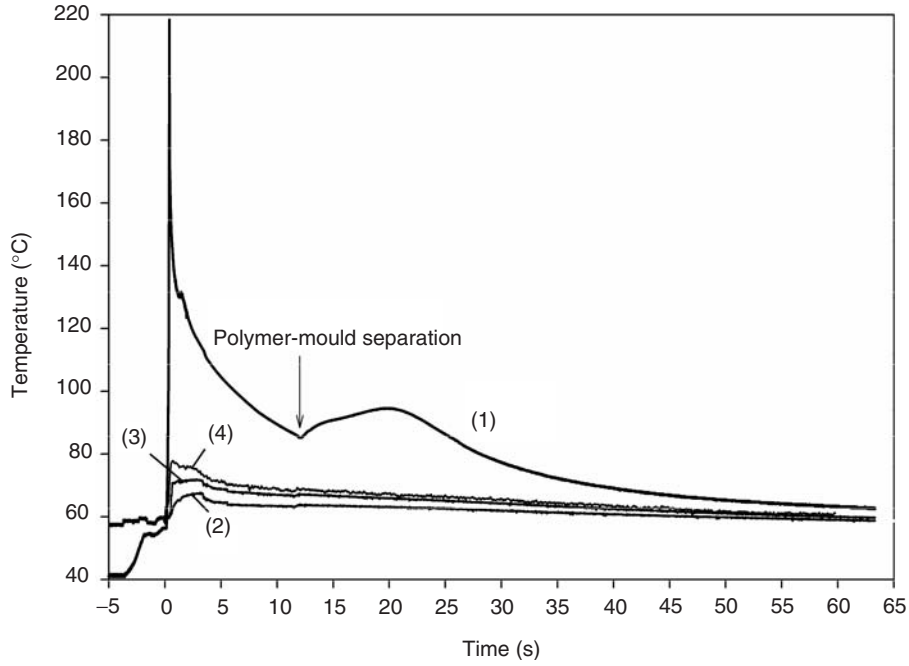

Figure 13 Temperature traces in the mould and at the surface of the polymer stream. (1): temperature at the surface of the polymer stream; (2): temperature in the mould at 2 mm from the interface; (3): temperature in the mould at 1 mm from the interface; (4): temperature at the surface of the mould calculated using Beck's method

resulting from the inverse calculation is reported in Figure 13 with curve 4. The surface temperature varied in time and increased by almost 20°C just after polymer injection. Hence, a constant mould temperature that is usually taken as boundary condition in injection moulding software may give rise to inaccurate heat transfer predictions. Furthermore, the heat flux that crossed the polymer–mould interface, also obtained from the inverse calculation, is reported via curve 1 in Figure 14. This evolution in time is typical of injection moulding cycles (Delaunay *et al.*, 2000; Ozisik, 1980; Shiraishi *et al.*, 2002). Heat fluxes are theoretically infinite when the polymer reaches the thermal probe and then decreases toward zero when the cooling of the part is achieved.

TCR history that resulted from the previously measured and calculated quantities is reported with curve 2 in Figure 14. The magnitude of TCR was in good agreement with results reported in the literature (Ozisik, 1980). At short times, TCR did not change as long as high pressure was maintained inside the cavity. When the cavity pressure dropped back to zero, a sudden rise in TCR was observed. The sudden rise of TCR was related to the appearance of the air gap caused by the polymer shrinkage.

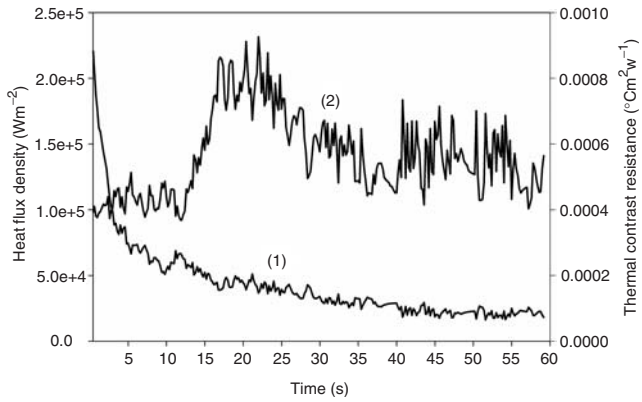

Figure 14 Surface heat flux (1) calculated using the internal temperatures provided by the two-thermocouple probe, and calculated TCR (2)

6. Conclusion

A new remote radiation thermometer has been designed for low-temperature monitoring in the injection moulding process. The radiometric procedure may also be employed in other applications such as extrusion and blow moulding. The key feature of the new system is the use of a special hollow optical fibre for transmitting the radiation emitted by the target to the photon detector. The advantage of the latter fibre is its high transmission in the mid- and far-infrared bands, which allows its use for low-temperature applications, whereas conventional full-core optical fibres exhibit high transmission loss in those spectral regions. Infrared optical fibres do exist but are very expensive, fragile and not suitable for low-temperature radiometry. The new radiometric device allows the measurement of the bulk temperature inside polymer streams. It is also specifically designed for surface temperature measurement of polymers that are opaque in the 3.4-m wavelength region. A similar system based on the same technology may be easily developed for surface temperature monitoring of polymers opaque in the 7.9-m wavelength region. Surface temperature is an extra piece of information that is provided for the first time in remote radiometry of injection moulding. Its knowledge gives a better insight into the nature of heat transfer at the polymer–mould interface. Moreover, it may be used to determine the detailed temperature profile through the stream thickness by using inverse problem algorithms. Extensive use of the new hollow optical fibre system in injection moulding has proven that it is an accurate and reliable instrument. Shrinkage and warpage phenomena effects that are usually encountered in such processes were clearly observed in the surface and bulk temperature histories.

References

Alaluft, M., **Dror, J.**, **Katzir, A.** and **Croitoru, N.** 1993: Infrared radiometry measurements using plastic hollow waveguides based on thin films. *Journal of Physics D: Applied Physics* 26, 1036–40.

Beck, J.V. 1986: Combined function specification-regularization procedure for solution of inverse heat conduction problem. *AIAA Journal* 24, 180–85.

Beck, J.V., **Blackwell, B.** and **St. Clair, C.R.** 1985: *Inverse heat conduction*. Wiley.

Bendada, **A**. and **Nguyen**, **K.T**. 1999: Inverse heat conduction of time and space dependent temperature during material processing. *3rd International Conference on Inverse Problems in Engineering*. ASME, 355–61.

Chervin, J.C., **Syfosse, G.** and **Besson, J.M.** 1994: Optical strength of sapphire windows under pressure. *Review of Scientific Instruments* 65, 2719–25.

Cossman, P.H., **Romano, V.**, **Sporri, S.**, **Altermatt, H.J.**, **Croitoru, N.**, **Frenz, M.** and **Weber, H.P.** 1995: Plastic hollow waveguides. *Lasers in Surgery and Medicine* 16, 66–75.

Delaunay, D., **Le Bot, P.**, **Fulchiron, R.**, **Luye, J.F.** and **Regnier, G.** 2000: Nature of contact between polymer and mold in injection molding. Part I: Influence of a non-perfect thermal contact. *Polymer Engineering and Science* 40, 1682–91.

Gannot, I., **Schrunder, S.**, **Dror, J.**, **Inberg, A.**, **Ertl, T.**, **Tschepe, J.**, **Muller, G.J.** and **Croitoru, N.** 1995: Flexible waveguides for Er-YAG laser radiation delivery. *IEEE Transactions on Biomedical Engineering* 42, 967–72.

Harrington, J.A. 2000: A review of IR transmitting hollow waveguides. *Fiber and Integrated Optics* 19, 211–27.

Konno, **M.**, **Cui**, **A.**, **Nishiwaki**, **N**. and **Hori**, **S**. 1993: *51st ANTEC Conference*. Society of Plastics Engineers, 2798–803.

Lai, G.Y. and **Rietveld, J.X.** 1996: Role of polymer transparency and temperature gradients in the quantitative measurement of process stream temperatures during injection molding via IR pyrometry. *Polymer Engineering and Science* 36, 1755–68.

Maier, C. 1996: Infrared temperature measurement of polymers. *Polymer Engineering and Science* 36, 1502–12.

Matsuura, Y. and **Harrington, J.A.** 1995: Infrared hollow glass waveguides fabricated by chemical vapor deposition. *Optics Letters* 20, 2078–80.

Migler, **K.B**. and **Bur**, **A.J**. 1997: Measuring temperature profiles during polymer processing. *Plastics Engineering* October, 27–29.

Migler, K.B. and **Bur, A.J.** 1998: Fluorescence based measurement of temperature profiles during polymer processing. *Polymer Engineering and Science* 38, 213–21.

Nguyen, K.T. and **Bendada, A.** 2000: An inverse approach of the prediction of the temperature evolution during induction heating of a semi-solid billet. *Modelling and Simulation in Materials Science and Engineering* 8, 857–70.

Ozisik, M.N. 1980: *Heat conduction*. Wiley, New York.

Quilliet, **S.**, **Le Bot**, **P.**, **Delaunay**, **D**. and **Jarny**, **Y.** 1997: Heat transfer at the polymer-metal interface. A method of analysis and its application to injection molding. *Proceedings of the National Heat Transfer Conference 2*. ASME, 9–16.

Reinhardt, H.J. 1993: Analysis of sequential methods of solving the inverse heat conduction problem. *Numerical Heat Transfer B* 24, 445–74.

Rietveld, **J.X**. and **Lai**, **G.Y**. 1994: Inverse method for obtaining the temperature profile within a mold cavity via IR pyrometry. *Proceedings of the ANTEC Conference*. Society of Plastics Engineers, 836–40.

Saito, M. and **Kikuchi, K.** 1997: Infrared optical fiber sensors. *Optical Review* 4, 527–38.

Saito, M., **Sato, S.** and **Miyagi, M.** 1992: Radiation thermometry for low temperatures using an infrared hollow waveguide. *Optical Engineering* 31, 1793–99.

Shiraishi, Y., **Norikane, H.**, **Narazaki, N.** and **Kikutani, T.** 2002: Analysis of heat flux from molten polymers to molds in injection molding processes. *International Polymer Processing* 2, 166–75.